analytical chemistry

Technical Note

pubs.acs.org/ac

Enhancing the Quality of H/D Exchange Measurements with Mass Spectrometry Detection in Disulfide-Rich Proteins Using Electron Capture Dissociation

Cedric E. Bobst* and Igor A. Kaltashov

Department of Chemistry, University of Massachusetts Amherst, Amherst, Massachusetts 01003, United States

Supporting Information

ABSTRACT: Hydrogen/deuterium exchange (HDX) mass spectrometry (MS) has become a potent technique to probe higher-order structures, dynamics, and interactions of proteins. While the range of proteins amenable to interrogation by HDX MS continues to expand at an accelerating pace, there are still a few classes of proteins whose analysis with this technique remains challenging. Disulfide-rich proteins constitute one of such groups: since the reduction of thiol−thiol bonds must be carried out under suboptimal conditions (to minimize the back-exchange), it frequently results in incomplete dissociation of disulfide bridges prior to MS analysis, leading to a loss of signal, inadequate sequence coverage, and a dramatic increase in the difficulty of data analysis. In this work, the dissociation of disulfide-linked peptide dimers produced by peptic digestion of the 80 kDa glycoprotein transferrin in the course of HDX MS experiments is carried out using electron capture dissociation (ECD). ECD results in efficient cleavage of the thiol−thiol bonds in the gas phase on the fast LC time scale and allows the deuterium content of the monomeric constituents of the peptide dimers to be measured individually. The measurements appear to be unaffected by hydrogen scrambling, even when high collisional energies are utilized. This technique will benefit HDX MS measurements for any protein that contains one or more disulfides and the potential gain in sequence coverage and spatial resolution would increase with disulfide bond number.

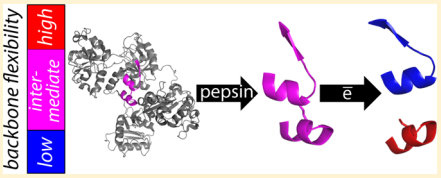

Hydrogen/deuterium exchange (HDX) with mass spectrometry (MS) detection has evolved in the past two decades into a powerful tool that is now used to decipher intimate details of processes as diverse as protein folding, recognition and binding, and enzyme catalysis.[1,2] While initially being a tool that was used exclusively in fundamental studies, HDX MS is now becoming an indispensable part of the analytical arsenal in the biopharmaceutical sector, where it is utilized increasingly in all stages of protein drug development from discovery to quality control.[3−5] Despite this progress, several areas remain where the application of HDX MS has met with only limited success. Disulfide-rich proteins constitute one such group, where characterization of higher-order structure and dynamics is particularly difficult, because of the suboptimal conditions used for reduction of thiol−thiol bonds following a quench of the exchange reactions. Proteins containing disulfide bonds are encountered very rarely in the protein folding studies where the most popular targets are small proteins lacking cysteine residues (with a notable exception of the oxidative folding studies), as well as in many other fundamental studies focusing on proteins of prokaryotic origin. However, disulfide-rich proteins are encountered very frequently in eukaryotic proteomes[6] and constitute a large segment of the biopharmaceutical products,[7] where the thiol−thiol bonds are critical elements defining conformation of protein drugs, and also play an important role in stabilizing proteins by endowing them with protease resistance.

While disulfide bond reduction is a relatively trivial task that can be readily accomplished at neutral pH using a variety of reagents, the acidic, low-temperature environment where proteins are placed to quench HDX narrows down the choice to a single reducing agent, TCEP.[8] However, the alkaline pH for optimal disulfide reduction by TCEP is substantially higher, compared to the acidic environment of typical "slow exchange conditions" commonly employed to minimize back exchange within proteins and their peptic fragments prior to MS analysis.[9] Furthermore, disulfide reduction in HDX MS measurements is usually carried out within a relatively short period of time (a few minutes) and at low temperature (0−4 °C) to limit the extent of the back-exchange, which in many situations does not allow the complete dissociation of thiol−thiol linkages of individual peptic fragments to be achieved in solution prior to LC separation and MS analysis of their deuterium content. Incomplete reduction of disulfide bonds dramatically increases the pool of candidate peptides that should be considered when analyzing proteolytic fragments in HDX MS measurements and frequently reduces sequence coverage and/or spatial resolution. While the former problem can be solved by employing more powerful and robust search engines for peptide identification, the latter one is more difficult to circumvent and can be very detrimental for the quality of HDX MS data and may require significant changes in experimental protocols. Indeed, a complete failure to reduce a certain disulfide bond in a protein will give rise to a thiol−thiol

Received: March 11, 2014
Accepted: May 12, 2014
Published: May 12, 2014

   dx.doi.org/10.1021/ac500904p | *Anal. Chem.* 2014, 86, 5225−5231

linked peptide dimer, whose constituent monomers do not necessarily represent a contiguous segment of the protein and may have vastly different conformational and dynamic properties. The total deuterium content of the entire dimer (measured by HDX MS) would not provide any meaningful information under these conditions, thereby effectively reducing the sequence coverage in the corresponding segments of the protein.

Certain changes in the sample work-up protocol in solution can alleviate this problem, at least for smaller proteins,[10] although it usually comes at a price of significantly increased levels of back exchange. An alternative approach to this problem examined in this work focuses on dissociation of disulfide-linked dimers in the gas phase to supplement (or replace) the reduction step in solution. Among several gas-phase ion fragmentation techniques that are capable of inducing the disulfide bond dissociation,[11,12] negative-ion collision-induced dissociation (CID)[13,14] and positive-ion ECD[15] (or its sister technique, electron transfer dissociation, ETD) have a particular appeal in that they can be implemented on most commercial instruments. While negative-ion CID has the additional advantage to perform measurements in a broad-band mode (without LC separation of peptic fragments),[16] its utilization as a means of inducing dissociation of disulfide bonds requires that very specific instrument types be used due to the sensitivity of the fragmentation channels to the collision energy. Perhaps more importantly, peptides tend to generate lower signal in the negative-ion mode, a feature that would certainly be detrimental to the quality of HDX MS data. In addition, it is unknown whether the high level of amide hydrogen scrambling observed within a model peptide under negative-ion CID[17] is also possible between two peptides linked by a disulfide. Therefore, this technique was excluded from the consideration in this work and the focus was shifted to an electron-based fragmentation method (ECD).

The suitability of ECD as a means of enhancing sequence coverage and spatial resolution that can be achieved in HDX MS studies of disulfide-rich proteins was evaluated in this work using the 80 kDa glycoprotein human serum transferrin (Tf) as a model system. Tf is a transport protein that is considered as a potential drug carrier, because of its unique ability to be internalized by cells in the process of endocytosis and cross physiological barriers in the process of transcytosis;[18,19] several Tf-based therapeutics are currently in development.[20−22] The proven therapeutic potential of Tf—its large size and the presence of multiple (18) disulfide bonds spread across the protein sequence—make it an epitome of modern protein drugs.[18] In this work, we used four partially overlapping disulfide-linked peptide dimers (Tf peptic fragments) to evaluate ECD as a tool to extract information on deuterium content of their constituent peptide monomers and examine the influence of hydrogen scrambling on the quality of these measurements. The results of this study provide clear evidence that dissociation of disulfide bonds in the gas phase by means of ECD leads to a noticeable improvement of both sequence coverage and spatial resolution, while hydrogen scrambling does not appear to affect the outcome of these measurements, even when ions experience relatively high levels of collisional activation.

MATERIALS AND METHODS

Human serum transferrin (Tf) was generously provided by Prof. A.B. Mason (University of Vermont, College of Medicine). Porcine pepsin and TCEP were purchased from Sigma−Aldrich Chemical Co. (St. Louis, MO), and D_2O was purchased from Cambridge Isotope Laboratories (Cambridge, MA). All other chemicals and solvents used in this work were of analytical grade or higher. Pepsin was immobilized onto a Poros 20 AL (Life Technologies, Grand Island, NY) support matrix, using the manufacturer suggested protocol and packed into a 2.1 × 50 mm column. Tf was digested in the absence of reductant under HDX quench conditions (pH 2.6, on ice) by running through the pepsin column at a flow rate of 0.1 mL/min, using a mobile phase of 0.1% formic acid. One hundred microliters (100 μL) of 2 μM Tf was injected for each run. Resulting peptides were concentrated and desalted on a peptide trap prior to their separation via reverse-phase HPLC (Agilent 1100 HPLC system) using a Jupiter 4 μm Proteo 90 Å 2 × 50 mm column (Phenomenex, Torrance, CA). HDX data were acquired using a rapid elution gradient (5−50% AcN in 0.1% formic acid in 5 min at 0.2 mL/min), whereas longer elution gradients (5−50% in 45 min) were utilized for peptide mapping purposes. Identification of the disulfide linked peptides was aided by liquid chromatography−tandem mass spectroscopy (LC-MS/MS) analysis of a set of peptides in which the cysteine thiol groups had been reduced and alkylated post-digestion. HDX was initiated by dilution into D_2O buffer (50 mM sodium phosphate pH 7.2) at 37 °C with a final H:D ratio of 1:10. All measurements were made on a solariX 7 Tesla Fourier-transform ion cyclotron resonance mass spectrometer (Bruker Daltonics, Billerica, MA) with a quadrupole front end. Precursor ions were mass-selected in the quadrupole filter using an isolation window of 10 m/z units and an accumulation time of 0.25 s. Peptides transmitted to the ICR cell were fragmented by electron capture dissociation (ECD), using a pulse length of 0.1 s and pulse bias of 1.0. Data were processed using DataAnalysis 4.0 (Bruker Daltonics, Billerica, MA), which allowed averaging of several adjacent ECD scans (typically 3−5 during HDX data acquisition) resulting from the same precursor ion. End-point samples were prepared by performing the exchange under acid denaturing conditions (in 0.88% formic acid) at 37 °C for 1 h and then adjusting the pH to 2.6 prior to digestion and analysis. Back exchange rates for the four peptides discussed in detail in this text varied from 25 to 32%, within the range typically observed with our setup (5−40%).

RESULTS AND DISCUSSION

Peptic digestion of Tf under HDX quench conditions that include a short incubation in a high concentration of TCEP produces a peptide map with poor coverage of Cys containing residues (Figure 1 in the Supporting Information). Of the 38 Cys residues in Tf, we are able to consistently detect less than one-fifth in their reduced form. Extending the preincubation to 10 min resulted in a modest improvement in the intensity of these seven peptides; however, we were not able to increase the number of free Cys detected. Peptic digestion of Tf under HDX quench conditions in the absence of reductant typically generates ∼340 peptide fragments of sufficient intensity for reliable HDX measurements. This number of peptides dramatically increases to 820 after extensive reduction of the sample with TCEP prior to LC-MS analysis, with 110 peptides being common to both datasets. While the peptides present in both reduced and nonreduced samples derive from protein segments that do not contain cysteine, the nonoverlapping part of the two sets represents disulfide-linked peptide dimers and higher multimers, as well as monomers with internal disulfides.

dx.doi.org/10.1021/ac500904p | Anal. Chem. 2014, 86, 5225−5231

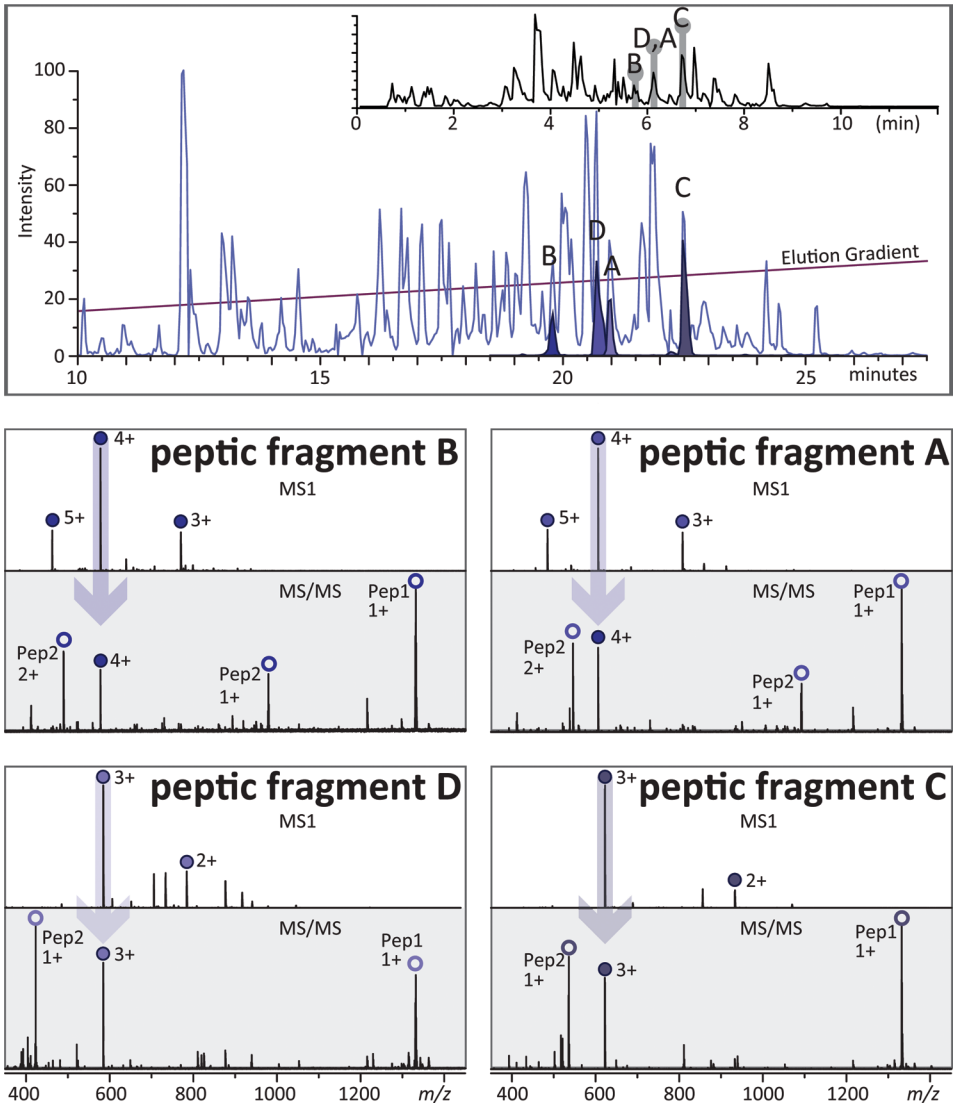

Figure 1. Identification of disulfide-linked peptide dimers by LC/MS/MS. The top diagram shows the total ion chromatograms (TIC) of the peptic fragments derived from Tf digested under conditions identical to those used in HDX MS experiments. The large TIC corresponds to the long elution gradient used to enhance separation of proteolytic fragments and identify the highest possible number of peptides and to increase the time window for MS/MS measurements. The smaller TIC inset above is an example TIC generated during HDX MS/MS data collection. Panels labeled A–D illustrate the identification of disulfide-linked peptide dimers by observing distinct peptide monomers following fragmentation of a precursor ion with ECD (extracted ion chromatograms for these four peptide dimers are indicated by corresponding letters A–D in both upper TIC traces).

Identification of these peptides is not a trivial task, because of the low specificity of protein hydrolysis by pepsin, which (coupled with the heterogeneity of the two carbohydrate chains and the possibility of having partial reduction of disulfides within cysteine-rich segments of the protein) leads an astronomically high number of "candidate" peptides. Matching up their calculated masses against the set of the measured masses requires computerized tools beyond what is typically offered by standard search engines. In our work, we identified candidate disulfide containing peptides by focusing on a pool of highly abundant peptic fragments unique to the nonreduced sample. Among these, disulfide linked peptides were readily identified by ECD using a long elution gradient and visually scanning the data for parent ions producing few dominant fragments.

This procedure is illustrated in Figure 1, where several related peptide dimers are identified by subjecting corresponding ions to ECD in the ICR cell. While numerous low-abundance fragments can be detected in each case, the two most prominent fragments consistently correspond to the dissociation of the external disulfide bond linking the two monomeric units. All four dimers share one monomeric unit, represented by the Val^{396}–Leu^{408} segment of the protein ("peptide 1" in Figure 1), while the second monomeric unit ("peptide 2" in Figure 1) corresponds to segments of varying length within Leu^{671}–Pro^{679}. While enhancing sequence coverage, the promiscuous sequence specificity of pepsin can also reduce peptide ion abundance in regions such as Leu^{671}–Pro^{679}, where multiple overlapping fragments are generated. Further loss in intensity would be caused by incomplete reduction of disulfides within such a region. This explains why peptide Val^{396}–Leu^{408}, common to the four disulfide linked peptides in Figure 1, was detected under reducing quench conditions (Figure S1 in the Supporting Information), whereas the linked counterparts containing residue Cys674 were not. An added benefit to utilizing disulfide linked peptides is the

dx.doi.org/10.1021/ac500904p | *Anal. Chem.* 2014, 86, 5225–5231

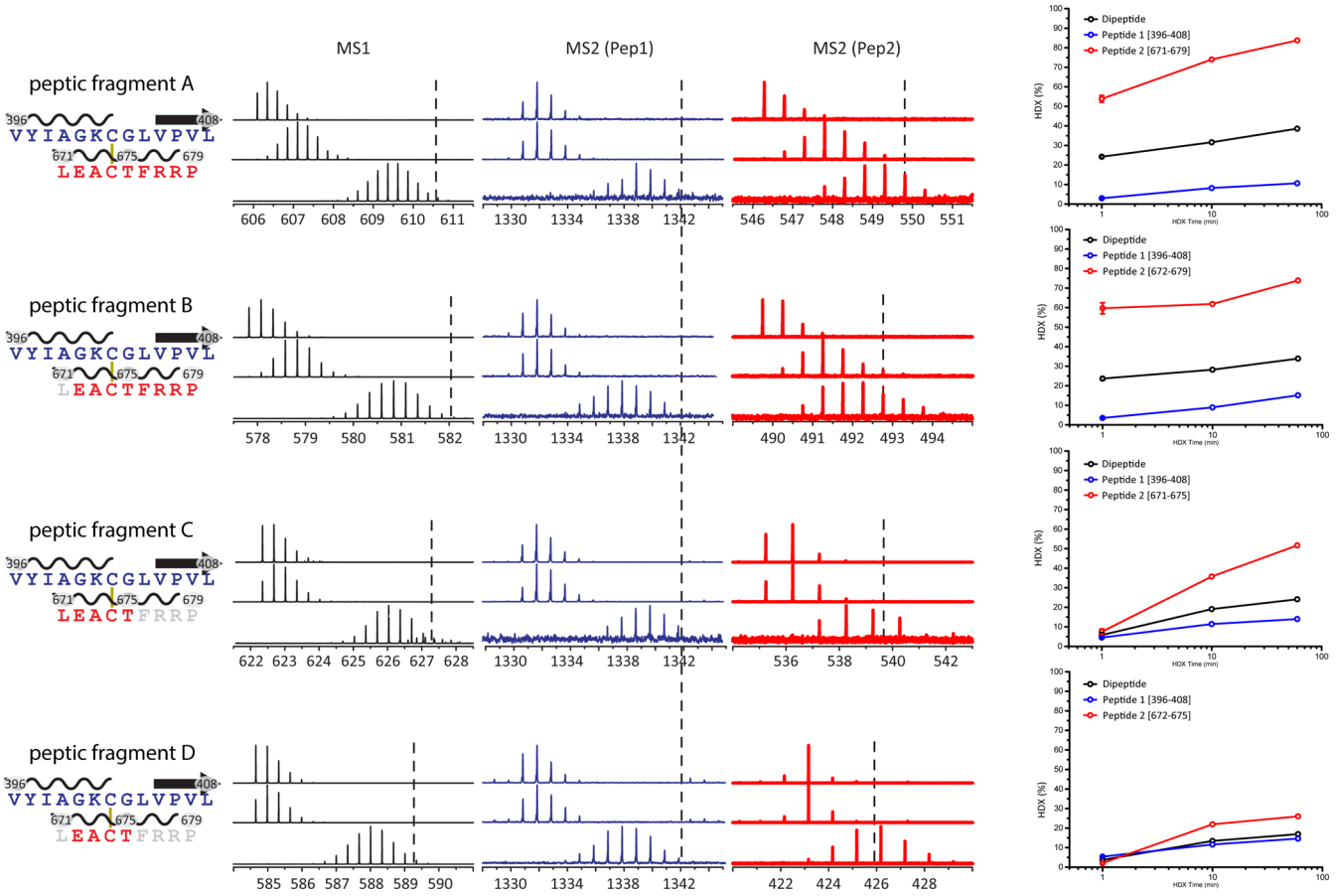

Figure 2. HDX MS and HDX MS/MS data for the four overlapping peptide dimers (structures are shown in the left column). The "MS1" column illustrates HDX MS measurements for each dimer (top trace: isotopic distribution of an unlabeled peptide ion, middle trace: isotopic distribution of the peptide following 1 min of exchange in solution, and bottom trace: end-point of the exchange reaction). The two "MS2" columns illustrate HDX MS/MS data for each monomeric constituent of the peptide dimer ("Pep 1" and "Pep 2"). The far right column shows kinetic plots for HDX MS (black trace) and HDX MS/MS (blue and red) measurements.

potential to detect small hydrophilic fragments not readily retained by RPLC in their reduced form. Complete chromatographic separation of the four example peptide dimers is problematic, even with the longer elution gradient used for peptide mapping in Figure 1 and overlapping elution profiles were observed for the rapid gradient of HDX MS measurements. Nevertheless, high efficiency of disulfide cleavages with ECD allows reproducible isotopic distributions to be obtained for each monomeric constituent with the quality that is more than adequate for HDX MS measurements. We chose these four disulfide-linked peptides as a model to evaluate the application of gas-phase disulfide cleavage in the HDX MS scheme; data for several other disulfide-linked peptides readily identified from the same sample are shown in the Supporting Information (Figures S2–S5). While all disulfide-linked species identified in the Tf peptic digest are currently limited to dimers (largely from their relative ease of identification), we have observed facile cleavage of disulfides in a linked peptide trimer and believe separation of even higher multimers is possible, perhaps at a reduced efficiency. Based on our observations, we find ECD effective at separating peptides linked by a single disulfide, while the efficiency of cleaving multiple disulfide bonds connecting two peptides remains to be evaluated.

HDX MS data obtained at the entire peptide dimer level for each of the four peptic fragments listed above (column labeled "MS1" in Figure 2) reflects the exchange averaged out across both constituents of the dimer. Since these monomeric units are noncontiguous in the protein sequence and, in fact, are located within very different structural elements of the protein, the averaged exchange data are not particularly meaningful. Although one can easily plot the time course of deuterium uptake for each of the dimer (black curves in the far right column in Figure 2), each curve is a convolution of contributions from two distinct parts. Therefore, it is not clear, for example, if the intermediate level of deuterium uptake exhibited by the peptide dimer (Val^{396}–Leu^{408})/(Leu^{671}–Pro^{679}) is a result of averaging out vastly different protection levels of the two monomers, or if the deuterium label is indeed distributed uniformly between the two monomers. The monotonically increasing overall protection within the series of the four dimers following the shortening of "peptide 2" does suggest that, in this particular case, one of the monomeric units (Val^{396}–Leu^{408}) is largely protected, while the other one has a significantly more dynamic character. Nevertheless, quantitative conclusions regarding the protection of each monomer are impossible to make, since even in the case of the shortest "peptide 2" (Glu^{672}–Thr^{675}, see the bottom diagram in Figure 2) the overall protection of the dimer is ca. 20%, which leaves the following possible protection ranges for its constituent monomers: 0 to 25% for "peptide 1" and 0 to 93% for "peptide 2."

dx.doi.org/10.1021/ac500904p | *Anal. Chem.* 2014, 86, 5225–5231

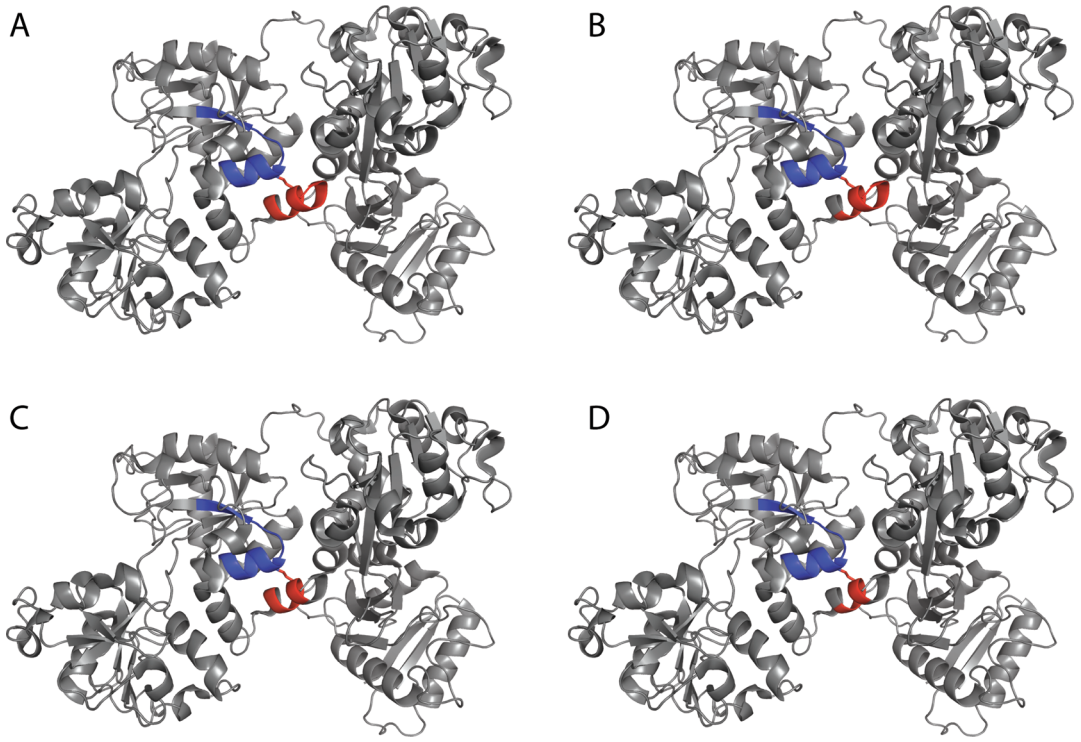

Figure 3. Location of the disulfide-linked peptide dimers characterized by HDX MS/MS within the crystal structure of Tf (PDB ID: 2HAV).

Inclusion of ECD in the HDX MS workflow as a means of separating the monomeric constituents of the disulfide-linked peptide dimers allows the deuterium content of each monomer to be measured individually. The results of these measurements are shown in the second and third columns of Figure 2. Despite the significant variation in the deuterium uptake levels exhibited by the intact peptide dimers, the isotopic distributions of "peptide 1" at each time point are very similar for all four precursor ions, and the slight variation is due to the different location of the exchange end points within this set. Once the end point variation is taken into account, the protection levels of "peptide 1" derived from different precursors become indistinguishable from each other within the experimental error (see the blue curves in Figure 2, far right column).

On the other hand, deuterium levels of "peptide 2" extracted from different precursor ions exhibit very significant variation: as the length of this segment is reduced from nine amino acid residues (Leu^{671}–Pro^{679}) to four (Glu^{672}–Thr^{675}), the relative deuterium uptake levels drop more than 3-fold (from nearly 80% for the longest peptide to 20% for the shortest, see the blue curves in Figure 2, far right column). This behavior is fully consistent with the observed variation in the deuterium protection within the set of four intact peptide dimers: as the protection level of the monomer with the fixed length (Val^{396}–Leu^{408}) remains constant within this set, increasing size of the second monomeric unit leads to its more dynamic character (via addition of amino acid residues exhibiting very low levels of amide protection), causing the overall protection at the dimer level to decrease.

The contrast between the exchange behavior of "peptide 1" extracted from four different dimer peptides and that of "peptide 2" is dramatic, but hardly surprising. Indeed, should the protection level of "peptide 1" be sensitive to the choice of a precursor ion, it would have clearly signaled that hydrogen scrambling is taking place. At the same time, the observed correlation between the length of "peptide 2" and the rate of deuterium uptake is noteworthy, as this variation must be attributed only to the vastly different exchange kinetics in solution exhibited by smaller segments and indeed single amino acid residues within (Leu^{671}–Pro^{679}). Locations of both Val^{396}–Leu^{408} (protein segment corresponding to "peptide 1") and Leu^{671}–Pro^{679} (the largest segment within the set of "peptide 2") within Tf are shown in Figure 3 (highlighted in blue and red, respectively). The first segment is composed of three different structural elements: a β-strand, an α-helix, and a short turn connecting them, with the latter component being the only element exposed to solvent, which explains the very low rate of deuterium uptake within this segment of Tf. In addition to being sequestered from solvent, the strand and the helix apparently reduce the flexibility of the connecting turn, thereby limiting amide exchange within this structural element as well. Unlike Val^{396}–Leu^{408}, Leu^{671}–Pro^{679} is a part of a single structural element of Tf, an α-helix (Figure 3).[23] Despite being fully structured in the crystallized form of Tf, this element is localized within the C-terminus of this protein, and is fully exposed to the solvent. Furthermore, two proline residues located within this helix are expected to weaken the internal network of hydrogen bonds stabilizing this element. The disulfide link connecting this helix to Val^{396}–Leu^{408} is the only "re-enforcer" of its structure besides the internal hydrogen bonds, and it is therefore not surprising that the residues located within the immediate vicinity of the cysteine residue (Cys^{674}) are much less flexible than the rest of this segment and, therefore, have much higher backbone amide protection (as reflected by the HDX MS measurements).

The data presented and discussed in the preceding paragraphs were collected under conditions that are typically used in HDX MS/MS experiments to minimize the extent of hydrogen scrambling in the gas phase. In general, these settings seek to minimize collisional activation of ions, as it has been

dx.doi.org/10.1021/ac500904p | *Anal. Chem.* 2014, 86, 5225–5231

shown to be a major factor contributing to hydrogen scrambling within protein and peptide ions prior to their dissociation by ECD.[24] However, the common "intra-chain" scrambling is not expected to affect the outcome of HDX MS/MS measurements presented in this work; only interchain proton hopping would result in alteration of the measured deuterium content of the fragments produced by dissociation of the disulfide bond. The possible role of collisional activation of peptide dimer ions as a trigger of interchain disulfide scrambling was examined by using a higher RF amplitude (1400 V vs 500 V) during isolation of precursor ions in the front-end quadrupole. Isotopic distributions for 1 min exchange data collected at the two different RF values were indistinguishable. Since collisional activation of peptide ions does not induce noticeable interchain scrambling, it is possible to use it as a means of enhancing the ionic signal prior to peptide dimer fragmentation if the experimental goal is to separate monomeric subunits by cleaving the disulfide bond in the gas phase. However, in this case, it might be impossible to use any other fragments (produced by cleavage of the backbone) to obtain site-specific information, since their deuterium content is likely to be altered by hydrogen scrambling.

Another opportunity to enhance the signal-to-noise ratio in measurements of the deuterium content of monomeric subunits within the peptide dimers might be offered by the recently introduced HDX MS/MS scheme where the LC step is eliminated from the work flow, using a continuous flow apparatus instead.[25,26] The desired level of the signal-to-noise ratio in this case is achieved by dramatically increasing the data acquisition window as the entire complement of peptic fragments generated under the slow exchange conditions are continuously infused into the ion source, and the high dynamic range and resolving power of FTICR MS are used to mass-select the peptide of interest for fragmentation under conditions that minimize hydrogen scrambling. This scheme might allow the deuterium occupancy to be probed at individual amides in addition to physically separating the monomeric subunits of peptide dimers. Finally, successful fragmentation of thiol−thiol linkages using ECD (or its sister technique ETD) under the conditions minimizing (or eliminating) hydrogen scrambling may also increase the range of proteins amenable to top-down HDX MS/MS analysis,[27] which is currently restricted to small proteins without disulfide bonds.[28−31]

CONCLUSIONS

Disulfide-rich proteins have traditionally been challenging targets for HDX MS studies, because of incomplete reduction of thiol−thiol linkages, which is a consequence of the quench conditions used to minimize amide back-exchange in peptides prior to MS analysis of their deuterium content: limited time, low temperature, and low pH. Traditionally, the principal strategy to address difficult-to-reduce or high-density disulfides in the HDX MS workflow is a brute force approach utilizing high concentrations of reductant and denaturant prior to (or even in combination with) digestion. The effectiveness of this approach is protein-dependent and extended incubation times frequently employed to enhance exposure to reductant invariably result in an undesirable increase in H/D back exchange. More recently, a novel electrochemical approach to reduce disulfides in solution under quench conditions prior to LC-MS has been reported for insulin.[32] While electrochemical reduction shows promise, several limitations were identified, an apparent requirement for low-salt conditions, a higher-than-optimal temperature (10 °C), and a current cell pressure limit of 50 bar. In this work, electron capture dissociation (ECD) was used to circumvent the disulfide problem, since it effectively cleaves external disulfide bonds. Dissociation of the disulfide-linked peptide dimers can be accomplished on the fast LC time scale and produces abundant signals for monomeric subunits without interchain hydrogen scrambling, even when collisional activation of ions is applied prior to ion selection and ECD fragmentation. Inclusion of ECD in the HDX MS workflow results in increased sequence coverage and spatial resolution and provides an attractive alternative to extensive chemical reduction of disulfide-rich proteins.

ASSOCIATED CONTENT

Supporting Information

Supplementary figures are provided as supporting information. This material is available free of charge via the Internet at http://pubs.acs.org.

AUTHOR INFORMATION

Corresponding Author

*Tel.: (413) 545-2888. Fax: (413) 545-4490. E-mail: cbobst@chem.umass.edu.

Notes

The authors declare no competing financial interest.

ACKNOWLEDGMENTS

This work was supported by a grant from the National Institutes of Health (No. R01 GM061666). Acquisition of the FTICR mass spectrometer was supported through the Major Research Instrumentation program with a grant from the National Science Foundation (No. CHE-0923329). The authors are grateful to Prof. Anne B. Mason (University of Vermont College of Medicine) for providing samples of human serum transferrin used in this work.

REFERENCES

(1) Englander, S. W. *J. Am. Soc. Mass Spectrom.* **2006**, *17*, 1481−1489.
(2) Konermann, L.; Pan, J.; Liu, Y.-H. *Chem. Soc. Rev.* **2011**, *40*, 1224−1234.
(3) Kaltashov, I. A.; Bobst, C. E.; Abzalimov, R. R.; Berkowitz, S. A.; Houde, D. *J. Am. Soc. Mass Spectrom.* **2010**, *21*, 323−337.
(4) Berkowitz, S. A.; Engen, J. R.; Mazzeo, J. R.; Jones, G. B. *Nat. Rev. Drug Discovery* **2012**, *11*, 527−540.
(5) Kaltashov, I. A.; Bobst, C. E.; Abzalimov, R. R.; Wang, G.; Baykal, B.; Wang, S. *Biotechnol. Adv.* **2012**, *30*, 210−222.
(6) Miseta, A.; Csutora, P. *Mol. Biol. Evol.* **2000**, *17*, 1232−1239.
(7) Walsh, G. *Nat. Biotechnol.* **2010**, *28*, 917−924.
(8) Burns, J. A.; Butler, J. C.; Moran, J.; Whitesides, G. M. *J. Org. Chem.* **1991**, *56*, 2648−2650.
(9) Cline, D. J.; Redding, S. E.; Brohawn, S. G.; Psathas, J. N.; Schneider, J. P.; Thorpe, C. *Biochemistry* **2004**, *43*, 15195−15203.
(10) Burke, J. E.; Karbarz, M. J.; Deems, R. A.; Li, S.; Woods, V. L.; Dennis, E. A. *Biochemistry* **2008**, *47*, 6451−6459.
(11) Chrisman, P. A.; McLuckey, S. A. *J. Proteome Res.* **2002**, *1*, 549−557.
(12) Mentinova, M.; Han, H.; McLuckey, S. A. *Rapid Commun. Mass Spectrom.* **2009**, *23*, 2647−2655.
(13) Bilusich, D.; Maselli, V. M.; Brinkworth, C. S.; Samguina, T.; Lebedev, A. T.; Bowie, J. H. *Rapid Commun. Mass Spectrom.* **2005**, *19*, 3063−3074.
(14) Bilusich, D.; Bowie, J. H. *Rapid Commun. Mass Spectrom.* **2007**, *21*, 619−628.

(15) Zubarev, R. A. *Curr. Opin. Biotechnol.* **2004**, *15*, 12−16.
(16) Zhang, M.; Kaltashov, I. A. *Anal. Chem.* **2006**, *78*, 4820−4829.
(17) Bache, N.; Rand, K. D.; Roepstorff, P.; Ploug, M.; Jorgensen, T. J. *J. Am. Soc. Mass Spectrom.* **2008**, *19*, 1719−1725.
(18) Kaltashov, I. A.; Bobst, C. E.; Zhang, M.; Leverence, R.; Gumerov, D. R. *Biochim. Biophys. Acta* **2012**, *1820*, 417−426.
(19) Kaltashov, I. A.; Bobst, C. E.; Nguyen, S. N.; Wang, S. *Adv. Drug Delivery Rev.* **2013**, *65*, 1020−1030.
(20) Yoon, D. J.; Chu, D. S. H.; Ng, C. W.; Pham, E. A.; Mason, A. B.; Hudson, D. M.; Smith, V. C.; MacGillivray, R. T. A.; Kamei, D. T. *J. Controlled Release* **2009**, *133*, 178−184.
(21) Pardridge, W. M. *Bioconjugate Chem.* **2008**, *19*, 1327−1338.
(22) Nguyen, S. N.; Bobst, C. E.; Kaltashov, I. A. *Mol. Pharmacol.* **2013**, *10*, 1988−2007.
(23) Wally, J.; Halbrooks, P. J.; Vonrhein, C.; Rould, M. A.; Everse, S. J.; Mason, A. B.; Buchanan, S. K. *J. Biol. Chem.* **2006**, *281*, 24934−24944.
(24) Rand, K. D.; Adams, C. M.; Zubarev, R. A.; Jorgensen, T. J. *J. Am. Chem. Soc.* **2008**, *130*, 1341−1349.
(25) Abzalimov, R. R.; Bobst, C. E.; Kaltashov, I. A. *Anal. Chem.* **2013**, *85*, 9173−9180.
(26) Pan, J.; Han, J.; Borchers, C. H.; Konermann, L. *Anal. Chem.* **2010**, *82*, 8591−8597.
(27) Kaltashov, I. A.; Bobst, C. E.; Abzalimov, R. R. *Anal. Chem.* **2009**, *81*, 7892−7899.
(28) Abzalimov, R. R.; Kaplan, D. A.; Easterling, M. L.; Kaltashov, I. A. *J. Am. Soc. Mass Spectrom.* **2009**, *20*, 1514−1517.
(29) Pan, J.; Han, J.; Borchers, C. H.; Konermann, L. *J. Am. Chem. Soc.* **2009**, *131*, 12801−12808.
(30) Pan, J.; Han, J.; Borchers, C. H.; Konermann, L. *Anal. Chem.* **2011**, *83*, 5386−5393.
(31) Wang, G.; Abzalimov, R. R.; Bobst, C. E.; Kaltashov, I. A. *Proc. Natl. Acad. Sci. U.S.A.* **2013**, *110*, 20087−20092.
(32) Mysling, S.; Salbo, R.; Ploug, M.; Jorgensen, T. J. *Anal. Chem.* **2014**, *86*, 340−345.